Sens. & Instrumen. Food Qual. (2007) 1:133–141
DOI 10.1007/s11694-007-9014-0

ORIGINAL PAPER

# Encapsulation of quantum dots and carbon nanotubes with polypyrrole in a syringe needle for automated molecularly imprinted solid phase pre-concentration of ochratoxin A in red wine analysis

**Yun Wei · Longhui Qiu · Craig Owen · Edward P. C. Lai**

Received: 20 March 2007 / Accepted: 5 June 2007 / Published online: 18 July 2007


**Abstract** Nanometer-sized semiconductor quantum dots (QDs with CdSe core and ZnS shell) and carbon nanotubes (CNTs with multi-walls) were encapsulated inside a stainless steel syringe needle by electrodeposition of polypyrrole (PPy). By cross-linking the PPy with ethylene glycol dimethacrylate (EGDMA) in the presence of ochratoxin A (OTA) as a template, molecularly imprinted polypyrrole (MIPPy) was formed on the nano-hybrid structure at an increased specific surface area. The MIPPy/CNTs/QDs-modified needle was readily adapted in an autosampler for micro-solid phase preconcentration (μSPP) of OTA from a red wine sample. After pulsed elution (PE) with 2% triethylamine (TEA), the OTA was determined by high performance liquid chromatography (HPLC) with fluorescence detection (FD). In comparison with MIPPy/CNTs, this new nano-hybrid structure of MIPPy/CNTs/QDs significantly improved the % recovery of OTA. The method, MIPPy/CNTs/QDs-μSPP-HPLC-FD, demonstrated that the MIPPy was truly a molecularly imprinted polymer (MIP) with specific recognition for OTA. All red wine matrix components could be differentially washed out, prior to accurate determination of the strongly bound OTA.

**Keywords** Quantum dots · Carbon nanotubes · Polypyrrole · Ochratoxin A · Molecularly imprinted polymer · Micro-solid phase preconcentration · Automated analysis

Y. Wei · L. Qiu · C. Owen · E. P. C. Lai (✉)
Ottawa-Carleton Chemistry Institute, Department of Chemistry, Carleton University, Ottawa, ON, Canada K1S 5B6
e-mail: edward_lai@carleton.ca

## Introduction

Nano-particulate materials have opened new avenues of sensing and instrumentation research. Quantum dots (QDs) are special semiconductor nano-crystals whose electrons occupy well defined discrete quantum states. Tremendous interest is developing in the use of QDs as fluorescent labels and probes for biochemical applications. QDs appeal to bioengineering because specific biomolecules on their surface determine the binding affinity [1], as afforded by the bioconjugation of a highly specific monoclonal antibody [2]. These glowing nano-crystals can be ferried to specific molecules on the cell surface [3] to achieve labeling of the transfected cells [4]. Rapidly, QDs are becoming the material of choice for a variety of analytical applications. Novel research may arise from their bulk, surface and colloidal properties. As the nano-crystals form during manufacture, their shape changes and every crystal begins to expose more edges and corners. In other words, QDs have more surface area on which to perform chemical reactions. These nano-crystals can potentially advance analytical applications that depend on surface chemistry [5]. In particular, QDs may increase the sensitivity of solid phase preconcentration (SPP) because of their enormous surface area-to-volume ratio [6] and specific surface area [7, 8]. Although QDs differ in sizes and surface structures, they have similar specific surface area (typically 120–150 $m^2/g$) for chemical interactions [9, 10]. Moreover, low non-specific binding has been shown at intermediate sizes [11]. In previous studies, QDs were immobilized on a polylysine-coated glass surface [12]. A thin-film of QDs-polymer mix was spin-coated onto a silicon substrate, thereby creating a hybrid device [13]. Alternatively, multi-walled carbon nanotubes (CNTs) are of interest for composite materials due to their good electronic properties and

high mechanical stability [14]. They are commercially available with the following specifications: external diameter = 10–30 nm, length = 0.5–50 μm, purity >95%, specific surface area = 4–100 $m^2/g$. The utilization of CNTs as building blocks for nanodevices can readily be realized. Hetero-junctions of QDs and CNTs could become better alternatives for the synthesis of nanoscale devices. Ravindran et al. presented a technique to integrate QD at the ends of CNTs and reported a novel CNT–QD–CNT heterostructure with detailed chemical and physical characterization of the heterojunctions [15].

Molecular imprinting is tantamount to creating a memory cavity which is capable of selectively and reversibly rebinding the template. Polypyrrole (PPy) is excellent for electrochemical preparation of molecularly imprinted polymers (MIPs) due to its stability under mild preparation conditions of room temperature and +0.85 V versus Ag/AgCl (even when a cross-linker is added). Conducting PPy is a biocompatible polymer matrix wherein biochemical molecules can be incorporated by way of doping. Functionalization with a wide range of bioorganic templates (such as ochratoxin A) is possible. Desirable properties such as a large surface area was achieved by electrodeposition of PPy on macroporous stainless steel frits [16], and molecularly imprinted polypyrrole (MIPPy) has been used to encapsulate CNTs inside the frit pores for selective micro solid phase preconcentration (μSPP) [17]. More interestingly, a syringe needle can be packed with MIPPy-encapsulated CNTs for μSPP [18].

In the present work, an integrated sampling/extraction/elution/injection device is optimized by developing a new way to immobilize various nano-sized sorbents in the autosampler needle [19]. Knowing that conductive PPy is technically a semiconductor, MIPPy can be effectively used as macromolecular glue to immobilize semiconductor QDs on the CNTs surface during electrodeposition. This binary-mixture approach is advantageous because QDs offer a larger surface area than what CNTs can provide. The CNTs were cylindrical in shape with diameters (d = 2r, ranging from 10 to 30 nm) and lengths ($\ell$, ranging from 0.5 to 50 μm). Hence, their surface area to volume ratio is calculated to be $(2\pi r^2 + \pi d\ell)/(\pi r^2\ell) = 2/r + 2/\ell = 2/(20\ \text{nm}) + 2/(5000\ \text{nm}) = 0.10004\ \text{nm}^{-1}$ on average. This can be compared with the surface area to volume ratio of $(4\pi r^2)/(4\pi r^3/3) = 3/r = 3/(5.0\ \text{nm}) = 0.6\ \text{nm}^{-1}$ on average for the quantum dots which were spherical in shape (with diameters ranging from 4.5 to 5.5 nm). It is now obvious why QDs will provide a larger surface area for micro solid phase preconcentration than CNTs on a per-volume basis. We decided to use a mixture of CNTs and QDs (instead of QDs alone) to help alleviate the problem of high back-pressure inside the syringe needle. The expected benefits would be a significantly larger total surface area and shorter diffusion distances for more effective μSPP of ultratrace ochratoxin A (OTA) in red wine. OTA is a mycotoxin produced by specific types of fungi in wine products; it is well known as a potent nephrotoxin, teratogen and carcinogen to humans [20]. The MIPPy/CNTs/QDs-modified needle can be mounted in an autosampler for sequential HPLC-FD analysis of red wine samples. Operator-free processing of red wine samples >0.5 mL containing OTA at <0.04 ppb concentration levels is feasible. Different elution strategies are programmable on the HPLC autosampler to verify that MIPPy is truly a MIP with specific recognition for OTA if all red wine matrix components can be differentially washed out.

## Experimental

### Reagents and materials

OTA, pyrrole (Py), ethylene glycol dimethacrylate (EGDMA) and triethylamine (TEA) were purchased from Sigma-Aldrich (Mississauga, ON, Canada). Tetrabutylammonium perchlorate (TBAP) was obtained from Fluka (Buchs, Switzerland). Acetonitrile and methanol were HPLC-grade solvents obtained from Caledon (Georgetown, ON, Canada). Ammonium hydroxide and ammonium chloride were supplied by Fisher Chemicals (Fairlawn, NJ, USA). About 18-MΩ cm distilled deionized water (DDW) was obtained from a Millipore Milli-Q water system (Bedford, MD, USA). Multi-walled carbon nanotubes (CNTs) with ~95% purity were obtained from Shenzhen Nanotech Port (Shenzhen, China). These CNTs were manufactured by catalytic decomposition of $CH_4$, with diameters ranging from 10 to 30 nm and lengths ranging from 0.5 to 50 μm. CdTe/CdS sodium mercaptoproprionate quantum dots (ADS620QD) were supplied by American Dye Source (Baie D'Urfe, QC, Canada). OTA standard solutions were prepared according to the procedure established by González-Peńas et al. [21]. Red wines were purchased from a local store in Ottawa.

### Preparation of MIPPy/CNTs/QDs-modified stainless steel syringe needle

About 100 μM OTA, 1.0% by weight of CNTs and 1.0% by weight of aggregated QDs were present in the pre-polymerization mixture when Py was electropolymerized within each 22-gauge, 1.5-inches-long (for a perfect fit to the autosampler) stainless steel syringe needle (BD, Franklin Lakes, NJ, USA). The concentrations of Py, TBAP and EGDMA were 0.1 M, 0.1 M and 0.2 M respectively in the pre-polymerization mixture with ace-

tonitrile as the solvent. For electrochemical preparation of MIPPy-encapsulated CNTs/QDs, the needle was filled with the pre-polymerization mixture (0.1 M Py, 0.1 M TBAP, 0.2 M EGDMA, 1% by weight CNTs) and then connected to serve as the working electrode. A platinum wire was used as the counter electrode, and an Ag/AgCl electrode was used as the reference electrode. A Stoneheart BC1200 high-performance potentiostat (Madison, CT, USA) was used to apply a constant potential of +0.85 to +1.00 V on the needle. The applied potential was switched off after 30 min of electropolymerization. This set-up for electropolymerization was the same as that detailed elsewhere [18]. Then, the needle was filled with another pre-polymerization mixture (0.1 M Py, 0.1 M TBAP, 0.2 M EGDMA, 1% by weight QDs) for electropolymerization over 15 min. Afterwards, the OTA template was removed by continually washing the MIPPy/CNTs/QDs-modified needle with 2% TEA in an HPLC mobile phase (20:80 v/v acetonitrile–ammonia buffer + 20 mM $NH_4Cl/NH_3$, pH 9.2) until no OTA breakthrough peak was observed in the HPLC-FD analysis of eluate aliquots.

## Autosampler system for MIPPy/CNTs/QDs-μSPP-HPLC-FD analysis

The HPLC instrument consisted of a solvent pump (Shimadzu LC-6A, Kyoto, Japan), an injector valve (Valco Cheminert VIGI C2XL, Houston, TX, USA) equipped with a 20-μL injection loop, a column (Phenomenex polymerX RP-1, pH stability 0–14, 5 μm, 250 × 4.6 mm, Torrance, CA, USA), a fluorescence detector (Water 470, Boston, MA, USA), an integrator (Spectra Physics 42900, San Jose, CA, USA) and a data acquisition system (PeakSimple, Torrance, CA, USA).

A Bio-Rad (Hercules, CA, USA) AS-100 HRLC automatic sampler was added to build an automated MIPPy/CNTs/QDs-μSPP-HPLC-FL analysis system. The sampler was equipped with a six-port injection valve, a 20-μL injection loop, and a tray of up to one hundred 1.5-mL sample vials. After removing the original autosampler needle, a short length of Nalgene connection tubing was used to mount up the MIPPy/CNTs/QDs-modified needle. It was necessary to equip the connection tubing with a septum that helped avoid sample leaking as well as minimize band broadening during the transfer of sample solution from the vial to the injection loop.

## Automated MIPPy/CNTs/QDs-μSPP-HPLC-FD analysis of red wine for OTA

A sample of 0.04–1.0 ppb (or ng/mL) OTA standard solution or spiked red wine was automatically pumped through the MIPPy/CNTs/QDs-modified needle at a flow rate of 0.1 mL/min. All samples were acidified with 1% HCl (by volume) to enhance the μSPP recovery of OTA. After washing with 200 μL of DDW to eliminate polar organics and HCl, the preconcentrated OTA was eluted with 200 μL of 2% TEA in HPLC mobile phase each time. The eluate was collected with an automated injection valve (equipped with a 20-μL injection loop) and immediately injected onto the HPLC-FD for chromatographic analysis. The HPLC analysis used 20:80 v/v acetonitrile–ammonia buffer (20 mM $NH_4Cl/NH_3$, pH 9.2) as the mobile phase at a flow rate of 1.0 mL/min. Fluorescence detection of OTA was performed at optimal excitation and emission wavelengths of 380 nm and 440 nm. The optimization of HPLC-FD analysis was based on Yu et al.'s work [22]. The pulsed elution (PE) with 2% TEA would be continued automatically until no OTA breakthrough was observed in the HPLC-FD analysis of eluates. The MIPPy/CNTs/QDs-modified needle was finally washed with 200 μL of DDW for surface re-conditioning.

## Measurement of total surface area by pulsed amperometry

The working electrode consisted of a MIPPy/CNTs/QDs-modified needle. A platinum wire was used as the counter electrode, and an Ag/AgCl electrode was used as the reference electrode. A special cell was constructed in the laboratory for the measurement of total surface area by pulsed amperometry, with the three electrodes connected to a PalmSens electrochemical analyzer (Palm Instruments, Houten, Netherlands) as illustrated in Fig. 1. For pulsed amperometric detection (PAD) analysis, the working electrode potential was pulsed between –0.2 V and +0.4 V over 0.2 s (as described by Gooding [23]) to alternate the polymer from a neutral to oxidized state when a $Na_2SO_4$ standard solution was running through the modified needle

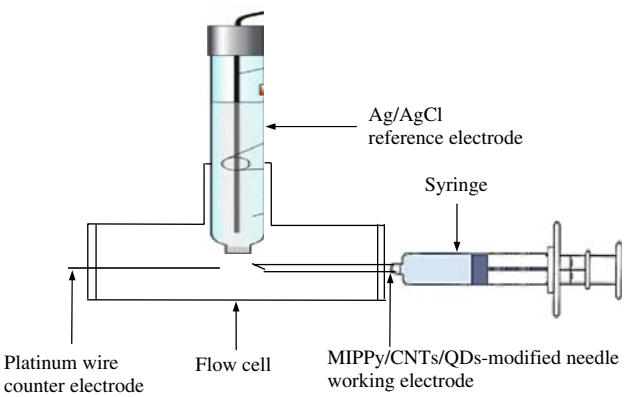


**Fig. 1** Schematic diagram of special cell constructed for measurement of total surface area by pulsed amperometry, with the three electrodes connected to PalmSens electrochemical analyzer

at a flow rate of 50 mL/h from a syringe pump. The PAD current was recorded every 1.0 s on a pocket PC (Hewlett-Packard Compaq iPAQ 3950, London, UK). A summary of the parameters used in PAD analysis is presented in Table 1. The pocket PC had a graphical user interface (PalmTime) that automatically plotted current versus time. This allowed the user to wait for the current (which indicated the total surface area) to stabilize until no fluctuations were observed. The pocket PC also stored the data in a file that could be transferred to a desktop computer for import to an Excel spread sheet.

## Results and discussion

### Preparation of MIPPy/CNTs/QDs-modified stainless steel needles

A blank stainless steel syringe needle would not bind OTA unless it was modified with a MIPPy film. In this work, MIPPy was electrochemically deposited to encapsulate CNTs and QDs on the inner wall of the needle for OTA binding. This was done according to the procedure reported by Yu and Lai [24]. The main components of the pre-polymerization mixture were Py, TBAP, EGDMA, CNTs and QDs. The monomer, Py, was chosen due to its high affinity for OTA. CNTs provided an extended 3-D framework inside the needle. They suspended well in the pre-polymerization solution and were good conductor of electricity for the electrodeposition of PPy (although it has previously been shown that overlapping of CNTs result in a decrease in their electronic conductance). QDs also have semi-conductive electronic properties that made them a good additional material to increase the total surface area, and hence OTA binding capacity, of the modified needle for μSPP. It was expected that MIPPy would form sheaths around the CNTs and QDs.

The process of molecular imprinting involved the interaction of Py monomers and OTA template molecules, whereby equilibrium of non-covalent bonds was created in the pre-polymerization solution. During electropolymerization, a positive potential of +0.85 V was applied from the potentiostat onto the stainless steel needle with respect to the Ag/AgCl reference electrode. This potential electrochemically oxidized Py, which then reacted with a neighboring monomer to form a chain [25]. The initiated polymerization was allowed to continue propagating for 30–90 min. According to Zhang and Bai, the oxidation potential of PPy is lower than that of the Py monomer [26]. Hence, MIPPy prepared by electrochemical polymerization was probably in its oxidized (or cationic) state and carried positive charges within the polymer. TBAP was the doping agent that provided a source of perchlorate anions during the polymerization process. They associated with the positively charged nitrogen atoms on the expanding MIPPy network. This balanced the positive charge of every nitrogen atom that formed as a result of the oxidative electropolymerization. EGDMA was used as a cross-linker to provide the structural support that enabled the newly formed MIPPy chains to have a tertiary structure. Without cross-linkers, the MIPPy chains would be too compact and binding interaction with OTA template molecules would be inhibited.

As previously demonstrated with MIPPy/CNTs, the CNTs were able to provide a rigid 3-D framework inside the stainless steel syringe needle [22]. The microstructure of MIPPy/CNTs/QDs composite films that was formed inside the modified needle (as illustrated in Fig. 2a) shows strong cohesion between MIPPy, CNTs and QDs. While the outer wall of the needle exhibited a smooth stainless steel surface, the inner wall of the needle was covered by a much rougher deposit of MIPPy-encapsulated CNTs and QDs. Teh et al. reported that the presence of CNTs provided more sites for nuclei formation such that there was extensive three-dimensional growth of PPy to attain greater surface roughness [27]. Another SEM image of MIPPy/CNTs/QDs-modified surface was obtained under high magnification of 15,000× (Fig. 2b). It reveals lots of cauliflower-like nodules (approximately 1 μm in size). This indicates that modification with MIPPy/CNTs/QDs dramatically increased the surface area of the stainless steel needle. We attribute this increase of surface area to the successful encapsulation of CNTs and QDs by MIPPy film which served as macromolecular glue.

After the electropolymerization, all OTA template molecules were removed from the MIPPy/CNTs/QDs network, creating the appropriate cavities specifically tailored for rebinding OTA. Every cavity would have the ideal size, shape, and orientation of functional groups to optimize

**Table 1** Parameters used in the PalmTime program (version 1.35) for PAD analysis

| Parameter | Setting | Description |
|---|---|---|
| E | –0.20 V | The constant potential applied. |
| E pulse | +0.40 V | The pulsed potential. |
| T pulse | 0.2 s | The duration of each potential pulse. |
| T interval | 1 s | The frequency at which the current was recorded. |
| T run | 100–400 s | This varied depending on desired duration of each run. |

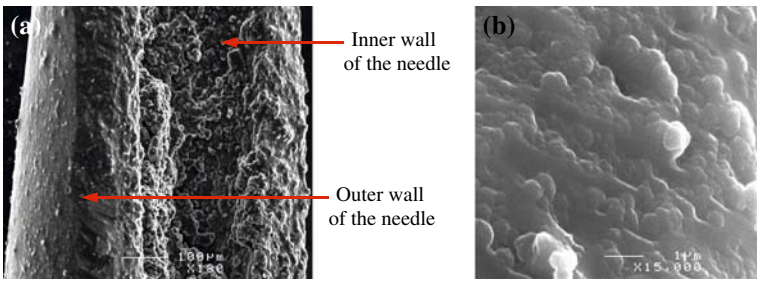


**Fig. 2** SEM images of a MIPPy/CNTs/QDs-modified stainless steel syringe needle tip

rebinding interactions. The atomic force microscope (AFM) would ideally be suited for characterizing nano-particles and -structures. It offers the capability of 3D visualization and qualitative/quantitative information on many physical properties including size, morphology, surface texture and roughness. Statistical information (including size, surface area, and volume distributions) can be determined as well. A wide range of particle sizes can be characterized in the same scan (from 1 nm to 8 μm). In addition, the AFM can characterize nanoparticles in multiple mediums including ambient air, controlled environments, and even liquid dispersions. Unfortunately, stainless steel needles (of the type used in this work) were not suited for AFM analysis because they lacked a flat surface in an accessible area.

## Improvement in % recovery of OTA

A sample solution was prepared by spiking 0.20 mL of 10 ppb OTA into 0.50 mL of filtered red wine, and then adding 0.30 mL of 1% HCl. The solution was run through the MIPPy/CNTs/QDs-modified needle, using the autosampler for μSPP, at a loading speed of 1.0 mL/h. After washing the needle with 600 μL of 1 M HCl, the bound OTA was eluted with 200 μL of 2% TEA for HPLC-FD analysis. Duplicate measurement of the OTA peak area yielded a 38 ± 1% recovery. This compares favorably with the 26 ± 1% recovery that was measured for a MIPPy/CNTs-modified needle (without any encapsulated QDs). These two results suggested that the QDs enhanced (by 1.5-fold) the total surface area available for μSPP inside the modified needle. Such a significant improvement was attained at the price of an amenable increase of back pressure during the μSPP step, which was well within the operational limits of the autosampler itself. Consequently, the detection limit was improved by 1.5-fold to reach a new low level of 0.02 ng/mL OTA in red wine analysis.

## Autosampler system for MIPPy/CNTs/QDs-μSPP-HPLC-FD analysis

All extraction parameters (such as the filling speed, filling volume, etc.) were programmed for direct control by the autosampler during MIPPy/CNTs/QDs-μSPP-HPLC-FD analysis. First, 1.0 mL of DDW was uploaded to pre-condition the MIPPy/CNTs/QDs-modified needle. Extraction of OTA was conducted by uploading 1.0 mL of OTA solution (at different concentrations, acidified with 1% HCl by volume) from a sample vial at a flow rate of 0.1 mL/min. During the extraction, the six-port injection valve was in the LOAD position (as illustrated in Fig. 3a). Hence the extraction procedure took 10 min to complete. Then, the sample loop and column were washed by the HPLC mobile phase (as illustrated in Fig. 3b) until no OTA peak was observed by the FD.

After washing the MIPPy/CNTs/QDs-modified needle with 0.1 mL of DDW, the pre-concentrated OTA was eluted by uploading 0.2 mL of 2% TEA (solution in mobile phase) from a sample vial at a flow rate of 1.0 mL/min while the six-port injection valve was in the LOAD position. Finally, the 2% TEA eluate was injected from the sample loop onto the HPLC column and the FD peak area for OTA was recorded. All the MIPPy/CNTs/QDs-μSPP-HPLC-FL analysis results for 1.5″ needles (shown in Fig. 4) were significantly better than those for 1.0″ needles (not shown). Unfortunately, 2.0″ needles would be too long to fit in the autosampler. Note that the expected benefits of a significantly larger total surface areas and shorter diffusion distances were realized for more effective μSPP of ultratrace ochratoxin A (OTA) in red wine, ultimately attaining nearly 100% recovery!

## Optimization of OTA template concentration in pre-polymerization mixture

In this study, OTA was used as the template, Py as the function monomer, and EGDMA as the cross-linker. The effect of OTA template concentration on the μSPP efficiency of MIPPy/CNTs/QDs-modified needle was investigated, as greatly facilitated by the automated HPLC-FD system. It was observed that the % recovery of 1.0 ng OTA (=1.0 mL × 1.0 ppb standard solution) was enhanced with increasing template concentration. When the template concentration was 75 μM, the recovery was only 76% ($n$ = 3, RSD = 3%); when the template concentration was increased up to 300 μM, the recovery dramatically increased to 95% ($n$ = 3, RSD = 3%) as shown in Fig. 5. These results clearly

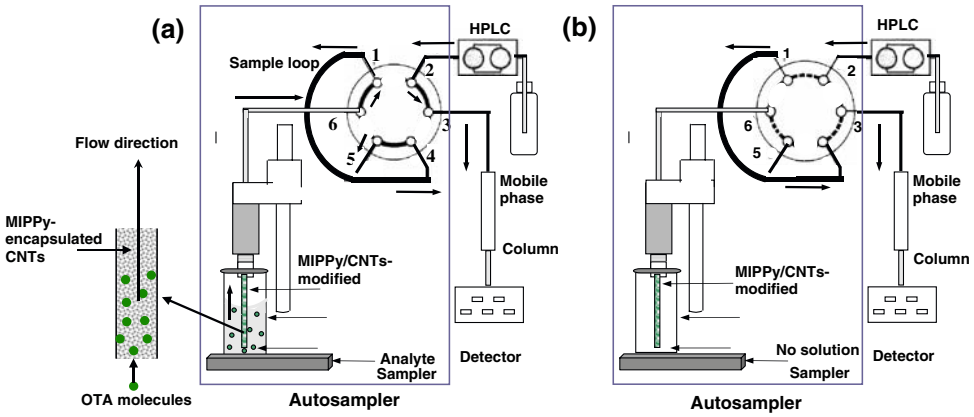


**Fig. 3** (**a**) Schematic diagram of automated MIPPy/CNTs/QDs-μSPP-HPLC-FD system in step 1 of μSPP procedure. MIPPy/CNTs/QDs-modified needle is uploading 1.0 mL of sample from vial. (**b**) Schematic diagram of automated MIPPy/CNTs/QDs-μSPP-HPLC-FD system in step 2 of μSPP procedure. Sample loop and column are being washed with HPLC mobile phase

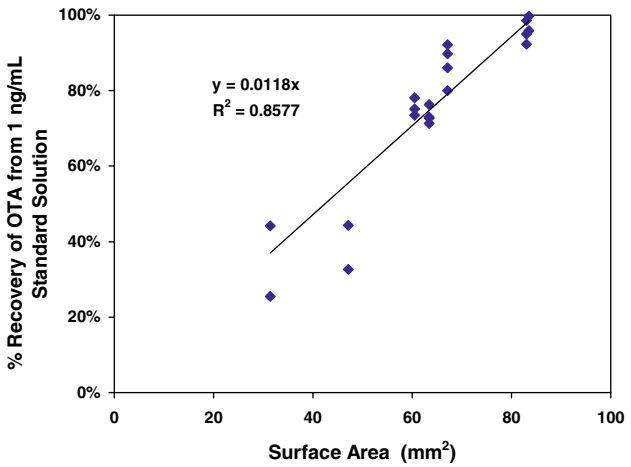


**Fig. 4** % Recovery of OTA from 1 ng/mL standard solution by MIPPy/CNTs/QDs-modified needles of different total surface areas

demonstrated that with an increase of available binding sites on the MIPPy/CNTs/QDs, the extraction efficiency (in terms of % recovery) was enhanced.

## Standard calibration curve for automated MIPPy/CNTs/QDs-μSPP-HPLC-FL analysis

A calibration curve was constructed from the peak area results obtained by MIPPy/CNTs/QDs-μSPP-HPLC-FD analysis of 1.0-mL OTA standard solutions using the automated system. As shown in Fig. 6, within the OTA concentration range from 0.02 to 1.50 ppb, the MIPPy/CNTs/QDs-μSPP-HPLC-FD peak area was linearly ($R^2 = 0.9990$) related to OTA concentration (or mass of OTA loaded on the MIPPy/CNTs/QDs-modified needle). The precision of MIPPy/CNTs/QDs-μSPP-HPLC-FD analysis was good, with a relative standard deviation under 6%. The time for automated sample processing by MIPPy/CNTs/QDs-μSPP was 16 min, which is significantly shorter than the 60 min typically required with the use of IAC columns.

## Measurement of total surface area by pulsed amperometry

A defining feature of CNTs and QDs is their large specific surface areas (SSA) [28], which is the surface area per unit mass. Specific surface area can indicate the average particle size, but not particle size range or distribution. Traditionally, gas absorption techniques such as Brunauer-Emmett-Teller (BET) analysis would be used to determine SSA. Instead of $N_2$ single point BET, electrochemical analysis was used in this work to measure the total surface area of each MIPPy/CNTs/QDs-modified needle. Conductive MIPPy/CNTs/QDs, in 0.1 M $Na_2SO_4$ electrolyte solution, allowed for amperometric measurement of the total surface area when an applied potential was pulsed between –0.2 V and +0.4 V versus the Ag/AgCl reference electrode [29]. A current signal was generated when the electrolyte was run through the MIPPy/CNTs/QDs-modified needle that served as a working electrode. The current was recorded over a short period of time for signal averaging. The average PAD current signal was compared with that obtained for a MIPPy-modified needle (without any encapsulated CNTs or QDs), as summarized in Fig. 7a. It became obvious that the encapsulation of CNTs/QDs increased the total surface area significantly. A PPy-modified needle served as the control for surface area measurement and for % recovery analysis. Further calibration of the PAD current versus the nominal surface area was made possible with the use of several commercially-available stainless steel syringe needles of different gauges and lengths, as presented in Fig. 7b.

## Automated MIPPy/CNTs/QDs-μSPP-HPLC-FD analysis of red wine

Due to the complexity of red wine matrix, one general problem in the HPLC-FD determination of OTA in red wine samples would be the interference from florescent matrix components (such as polyphenols). As shown in Fig. 8b, the large peaks from different components in red

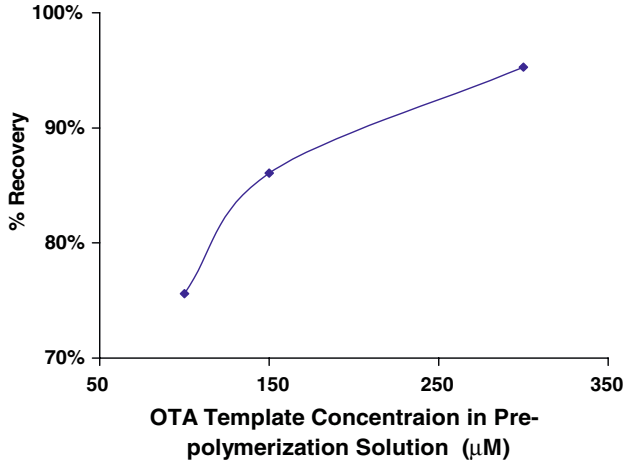


**Fig. 5** Effect of OTA template concentration on μSPP efficiency of MIPPy/CNTs/QDs-modified needle. Each data point represents the mean of triplicate measurements

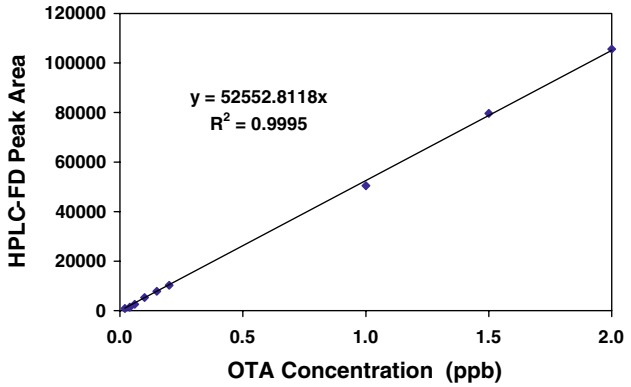


**Fig. 6** Standard calibration curve of automated MIPPy/CNTs/QDs-μSPP-HPLC-FD. Each data point represents the mean of duplicate measurements

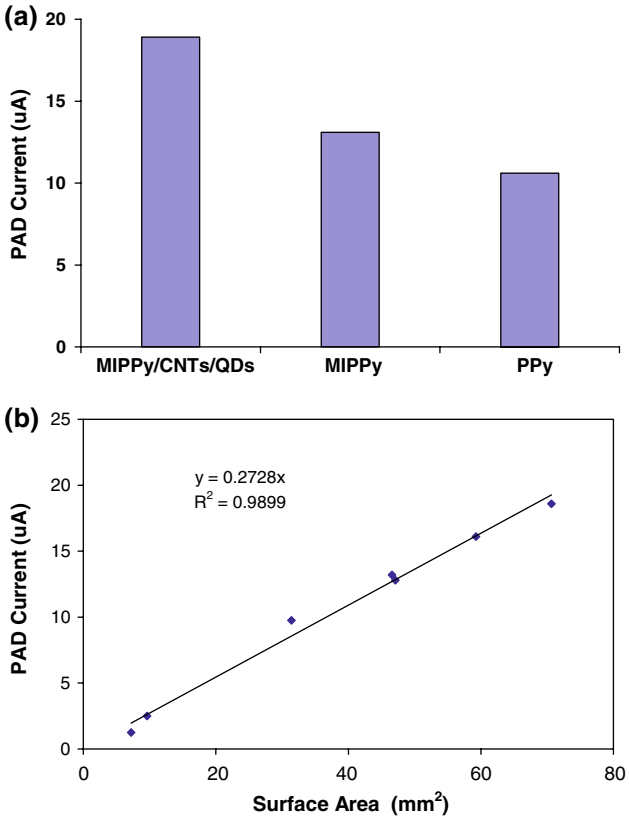


**Fig. 7** (**a**) Comparison of PAD currents measured for MIPPy/CNTs/QDs-modified needle, MIPPy-modified needle, and PPy-modified needle. (**b**) Calibration of PAD current versus nominal surface area of commercially-available stainless steel syringe needles of different gauges and lengths

wine matrix made quantitative interpretation very difficult in direct analysis of the 0.5 ppb-OTA-spiked red wine. The discrimination ability should be greatly enhanced, if these components are selectively removed before introduction of red wine sample to the HPLC instrument for analysis. Unfortunately, sample cleanup by commercial SPE cartridge tended to remove both OTA and matrix components indiscriminately. Varelis et al. even reported overload of the detector caused by the co-extracted polyphenols [30]. In our work, MIPPy/CNTs and MIPPy/CNTs/QDs modified stainless steel needles were employed to preconcentrate OTA from red wine matrix, thereby cleaning up the sample. Relatively clean chromatograms were obtained from both MIPPy/CNTs-μSPP-HPLC-FD analysis (Fig. 8c) and MIPPy/CNTs/QDs-μSPP-HPLC-FD analysis (Fig. 8d) after enrichment of OTA from 0.5 mL of 0.5 ppb-OTA-spike red wine. The results demonstrated that MIPPy/CNTs-μSPP and MIPPy/CNTs/QDs-μSPP were able to resolve OTA peaks from the red wine matrix components. Potential interference from the matrix components was thus greatly decreased. The chromatograms show that MIPPy/CNTs/QDs, with its larger total surface area, extracted both more OTA and more matrix components than MIPPy/CNTs.

The % recovery results of red wine matrix components and OTA from MIPPy/CNTs/QDs, MIPPy/CNTs and MIPPy/CNTs/QDs are compared in Fig. 9. Recoveries of red wind matrix components were calculated by comparing the red wind matrix peak areas from direct HPLC analysis of spiked samples and after μSPP enrichment of spiked samples with the modified needles. Note that the MIPPy/CNTs/QDs-modified needle afforded the highest OTA recovery of 61 ± 2% and a modest 9% recovery of red wine matrix components (same as the PPy/CNTs/QDs-modified needle) due to non-specific binding. Using the ratio of % recovery results between the red wine matrix components and the OTA as an alternative indicator of selectivity (data not shown), it strongly suggests that better selectivity towards the target OTA molecules was the benefit of molecularly imprinting done for the two MIPPy modified needles.

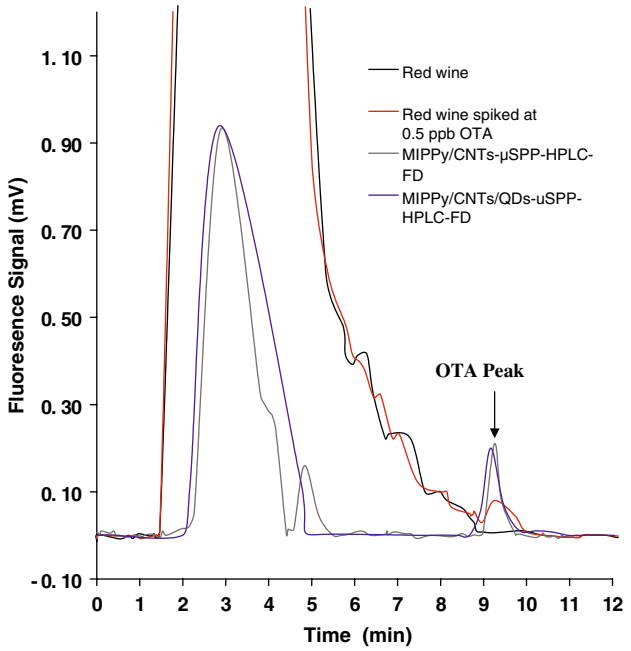


**Fig. 8** (**a**) Direct HPLC-FD analysis of red wine (black line). (**b**) Direct HPLC-FD analysis of red wine spiked at 0.05 ppb OTA (red line). (**c**) MIPPy/CNTs-μSPP-HPLC-FD analysis after enrichment of OTA from 0.5 mL of red wine spiked at 0.05 ppb OTA (grey line). (**d**) MIPPy/CNTs/QDs-μSPP-HPLC-FD analysis (using needle # 14) after enrichment of OTA from 0.5 mL of red wine spiked at 0.05 ppb OTA (blue line). All red wine samples were acidified with 1 M HCl (1% by volume) to provide nearly quantitative recovery of OTA for μSPP. After washing with 200 μL of DDW to eliminate polar organics and HCl, the pre-concentrated OTA was eluted with 100 μL of 1% TEA in the HPLC mobile phase

## Elimination of non-specific binding of red wine matrix components with MIPPy/CNTs/QDs

Previously the concept underpinning MIP theory was often exemplified by the lock-and-key model [31], based on enzyme-substrate interactions in biochemistry. X-ray diffraction later refuted this concept, showing that enzymes sustain a more flexible structure than synthetic MIPs. Nevertheless, MIPs are more thermodynamically stable and cost effective than their biological counterparts. They can be relatively easy to make and can be stored for many years without losing their structural integrity. One question we asked ourselves was: Is MIPPy/CNTs/QDs truly a new MIP in this nano-structured device (of modified syringe needle)? To investigate this issue, differential pulsed elution (DPE) was employed, which had been described in our previous reports To investigate this issue, differential pulsed elution (DPE) was employed, which had been described in our previous reports [32, 33]. DPE involved intermediate wash steps that would remove much of the weakly bound wine matrix components from the MIPPy/CNTs/QDs-modified needle. In our previous work on MIPPy/CNTs-modified stainless steel frits, several organic solvents were evaluated for their DPE effectiveness by using 100 μL of each solvent to wash the frit before PE-HPLC-FLD analysis [22]. In this study, 200 μL of 1 M HCl was used to wash the MIPPy/CNTs/QDs-modified needle before PE with 2% TEA. Ideally, DPE must eliminate all the wine matrix components quantitatively while keeping a good amount of OTA in the needle for subsequent HPLC-FL analysis. As shown in Fig. 10, weakly bound wine matrix components were totally eluted during the first three DPEs with 1.0 M HCl (total volume = 600 μL), while the strongly bound OTA was kept on the MIPPy/CNTs/QDs-modified needle. This new finding looked promising because a clean chromatogram was obtained without any interference of red wine components. The OTA peak (retention time = 6.4 min) was totally resolved down to the baseline. Now we know for sure that this MIPPy on CNTs/QDs was truly a new MIP!

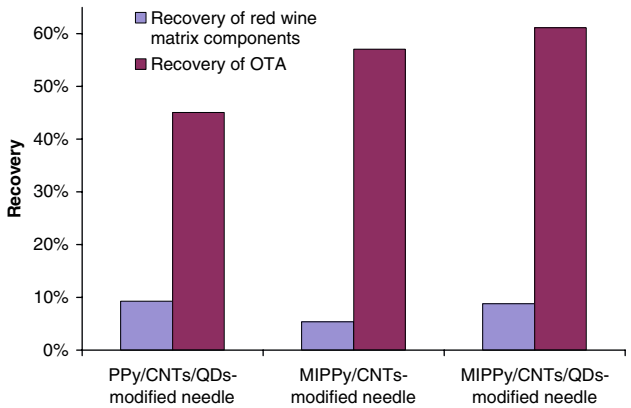


**Fig. 9** Recoveries of red wind matrix components and OTA using MIPPy/CNTs- and MIPPy/CNTs/QDs- modified needles. Data from a non-imprinted PPy/CNTs/QDs-modified needle are included for comparison

## Conclusions

A new μSPP device has been developed using MIPPy-encapsulated CNTs and QDs as the sorbent to attain a significantly larger total surface area. The MIPPy/CNTs/QDs composite was grown using electrochemical polymerization, in which the conductive polymer, nanotubes and quantum dots were simultaneously deposited along the inner wall of the stainless steel syringe needle to form a three-dimensional network. The resulting needle exhibited a significant enhancement of binding capacity (and % recovery) for OTA, as well as some effectiveness to remove the interfering components of a complex red wine matrix. The MIPPy/CNTs/QDs-modified needle as a μSPP device afforded an enriched sample that was suitable for sensitive determination of OTA by HPLC-FD. This new

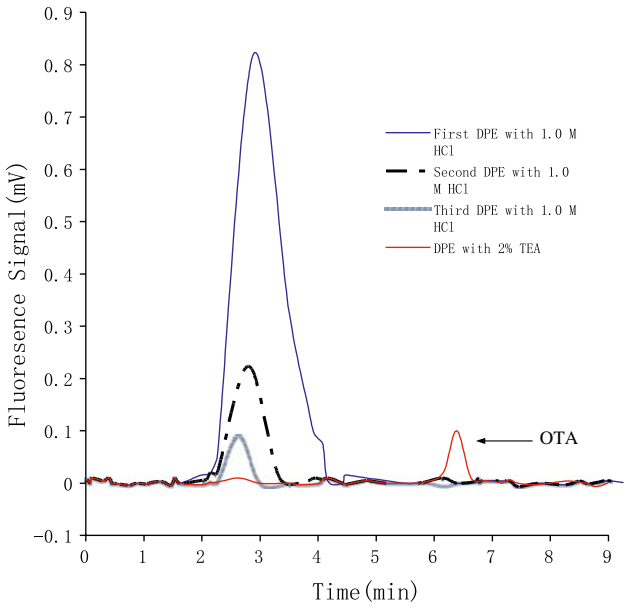


**Fig. 10** HPLC-FD analysis of (**a**–**c**) differential pulsed elution (DPE) of red wine matrix components with 3 × 200 μL of 1.0 M HCl, and (**d**) final pulsed elution (FPE) of OTA with 1 × 200 μL of 2% TEA

μSPP procedure could readily handle larger volumes (up to 10 mL) when an autosampler was operated. Automation of the μSPP-HPLC-FD procedure afforded rapid determination of ultratrace OTA. It is commonly believed that both the acceptance and the range of potential applications for a new technique with automation can be significantly promoted.

These newly developed MIPPy/CNTs/QDs-modified needles will be evaluated for the μSPP processing of various food samples, prior to their reverse-phase or size-exclusion liquid chromatography for the control of food quality and the monitoring of food safety. With further development of nano-particulate materials to open new avenues for sensing and instrumentation research, we will truly be on the verge of a major technological breakthrough that can have far-reaching impacts to all aspects of food science and engineering.

**Acknowledgements** Financial support of the Natural Sciences and Engineering Research Council (NSERC) Canada is gratefully acknowledged.

## References

1. www.nature.com/nprot/journal/v1/n3/full/nprot.2006.184.html
2. www.physorg.com/news536.html
3. www.sciencemag.org/cgi/content/full/300/5616/80
4. www.sciencemag.org/cgi/content/full/307/5709/538
5. J.M. Perkel, Scientist **16**, 32–34 (2002)
6. scienceweek.com/2003/sw030321.htm
7. materials.globalspec.com/.../Electrical_Optical_Specialty_Materials /Nanomaterials_Nanotechnology_Products - 60k –
8. www.nature.com/nmeth/journal/v1/n1/full/nmeth032.html
9. www.cdc.gov/niosh/topics/nanotech/safenano/healthconcerns.html
10. E.H. Sargent, Adv. Mater. **17**, 515–522 (2005)
11. www.mrs.org/s_mrs/bin.asp?CID=2629&DID=61013&DOC=FILE.PDF
12. X. Gao, W.C.W. Chan, S. Nie, J. Biomed. Opt. **7**, 532–537 (2002)
13. http://www.esm.psu.edu/news/item/274
14. P.G. Su, Y.L. Sun, C.C. Lin, Sensor. Actuat. B Chem. **115**, 338–343 (2006)
15. S. Ravindran, K.N. Bozhilov, C.S. Ozkan, Carbon **42**, 1537–1542 (2004)
16. J.C.C. Yu, S. Krushkova, E.P.C. Lai, E. Dabek-Zlotorzynska, Anal. Bioanal. Chem. **382**, 1534–1540 (2005)
17. J.C.C. Yu, E.P.C. Lai, React. Funct. Polym. **66**, 702–711 (2006)
18. Y. Wei, L. Qiu, J.C.C. Yu, E.P.C. Lai, Molecularly imprinted solid phase extraction in a syringe needle packed with polypyrrole-encapsulated carbon nanotubes for determination of ochratoxin A in red wine, Food Sci. Technol. Int., in press
19. A. Wang, F. Fang, J. Pawliszyn, J. Chromatogr. A **1072**, 127 (2005)
20. C. Brera, J.M. Soriano, F. Debegnach, M. Miraglia, Microchem. J. **79**, 109–113 (2005)
21. E. González-Peñas, C. Leache, M. Viscarret et al., J. Chromatogr. A **1025**, 163–168 (2004)
22. Jorn C.C. Yu, Edward P.C. Lai, Determination of ochratoxin A in red wines by multiple pulsed elutions from molecularly imprinted polypyrrole, Food Chem., accepted (November 15, 2006)
23. J.J. Gooding, C. Wasiowycha, D. Barnett, D.B. Hibbert, J.N. Barisci, G.G. Wallace, Biosens. Bioelectron. **20**, 260–268 (2004)
24. J.C.C. Yu, E.P.C. Lai, Anal. Bioanal. Chem. **381**, 948–952 (2005)
25. S. Sadki et al., Chem. Soc. Rev. **29**, 283–293 (2000)
26. X. Zhang, R. Bai, Langmuir **19**, 1073–1079 (2003)
27. Kwok-Siong. Teh, Liwei Lin, J. Micromech. Microeng. **15**, 2019–2027 (2005)
28. icon.rice.edu/resources.cfm?doc_id=4394
29. J.J. Gooding, C. Wasiowych, D. Barnett, D.B. Hibbert, J.N. Barisci, G.G. Wallace, Biosens. Bioelectron. **20**, 260–268 (2004)
30. P. Varelis, S.L. Leong, A. Hocking, G. Giannikopoulos, Food Addit. Contam. **23**, 1308–1315 (2006)
31. J.O. Mahoney, K. Nolan, M.R. Smyth, B. Mizaikoff, Anal. Chim. Acta **534**, 31–39 (2005)
32. W.M. Mullett, E.P.C. Lai, Microchem. J. **61**, 143–155 (1999)
33. S.Y. Feng, E.P.C Lai, E. Dabek-Zlotorzynska, S. Sadeghi, J. Chromatogr. A. **1027**, 155–160 (2004)